ISSN 1070-3284, Russian Journal of Coordination Chemistry, 2023, Vol. 49, No. 9, pp. 565–576. © Pleiades Publishing, Ltd., 2023.
Russian Text © The Author(s), 2023, published in Koordinatsionnaya Khimiya, 2023, Vol. 49, No. 9, pp. 553–564.

Nitro-Substituted Pyridinimine Complexes of Pd(II): Synthesis and Inhibition of MAO-B *ex vivo*

M. S. Denisov[a], *, ** and Yu. A. Beloglazova[a]

[a] *Institute of Technical Chemistry of Ural Branch of the RAS, Perm, Russia*

**e-mail: denisov.m@itcras.ru*

***e-mail: m189@mail.ru*

Received January 25, 2023; revised March 30, 2023; accepted April 6, 2023

Abstract—The first ever synthesis of complexes $[PdLCl_2]$ (**I**) and $[PdLBr_2]$ (**II**) was successfully achieved, where L = 2,6-dimethyl-4-nitro-*N*-(pyridin-2-ylmethylildene)aniline, a ligand with a purported ability to inhibit monoamine oxidase B (MAO-B). To gain insight into the molecular structure of complexes **I** and **II**, as well as the ligand precursor 2,6-dimethyl-4-nitroaniline L^4 (CIF files CCDC nos. 2255106 (**I**), 2255105 (**II**), 2255103 (L), 2255104 (L^4)), X-ray diffraction analysis was utilized. Complex **I** underwent further characterization to determine its stability, solubility, and lipophilicity. Cytotoxicity studies of substances L, **I**, and **II** on human embryonic kidney cell line HEK-293 showed no evidence of cytotoxic activity. To evaluate the inhibitory activity of new substances L, **I**, and **II** as well as established substances **III**–**IX**, selegiline, and rasagiline, *ex vivo* studies were conducted, establishing a structure/activity relationship.

Keywords: palladium, MAO, pyridinimine complexes, nitroaniline, Schiff base

DOI: 10.1134/S1070328423600626

INTRODUCTION

The growing interest in coordination compounds of transition metals is driven by the clinical use of Pt(II) complexes such as cisplatin and carboplatin in antitumor therapy [1–3]. However, the development of chemoresistance in cancer cells and the appearance of specific side effects in patients have prompted researchers to synthesize compounds based on Pd, owing to the similar chemical and physical properties of Pt and Pd [4]. Pd(II) compounds display significant antitumor and antimicrobial activity, higher lipophilicity, or solubility when compared to cisplatin [5–11]. The cytotoxic activity of Pd(II) complexes is dependent on the ligand environment, and can be purposefully reduced with individual selection and variation of the structure of the ligand. This feature expands the potential for application of Pd(II) complexes in the therapy of a number of infectious and non-infectious diseases [12–14].

Organometallic compounds have been identified as potential inhibitors of enzyme activity due to their high affinity for binding with large biological molecules when compared to organic compounds without metals [15]. Numerous studies have revealed that Pd(II) and Pd(IV) complexes possess inhibitory effects towards various enzymes such as AChE [16–19], BuChE [19, 20], PON1 [21], CA [16], α-glucosidase [18, 21], β-glucuronidase [22], cellulase [23], fumarate reductase [24], cathepsin B [25], TcOYE [26], HIV-1 protease [27], metallo-β-lactamase [28], RNA polymerases [29], lipoxygenase [30], superoxide dismutase [31], topoisomerase II [32], Na^+/K^+-ATPase [33], Ca^{2+}/Mg^{2+}-ATPase [34], thioredoxin reductase [35] and glutathione reductase [36].

Alzheimer's and Parkinson's diseases are neurodegenerative disorders that manifest in an age-dependent manner, and are known to exhibit increased activity of AChE [16–19] and MAO-B [37–39] enzymes, respectively. Presently, a variety of MAO-A and MAO-B inhibitors with distinct modes of action are available [38]. Notably, Moshkovsky's team demonstrated the potential of Pd(II) complexes to inhibit the enzymes MAO-A and MAO-B [40]. The cysteine residue 397 within the MAO polypeptide chain forms a covalent bond with FAD, which serves as the catalytic center of the enzyme [37, 38]. Pd complexes form aldimines in the reaction that converts monoamines by the MAO enzyme, thereby inhibiting it [41]. Mechanisms of catalytic action and inhibition of the MAO enzyme are depicted in Scheme 1. In a recent exploration [42], the effectiveness of MAO-B inhibition in the treatment of Parkinson's disease was found to be linked with the cessation of gamma-aminobutyric acid (GABA) synthesis by astrocytes.

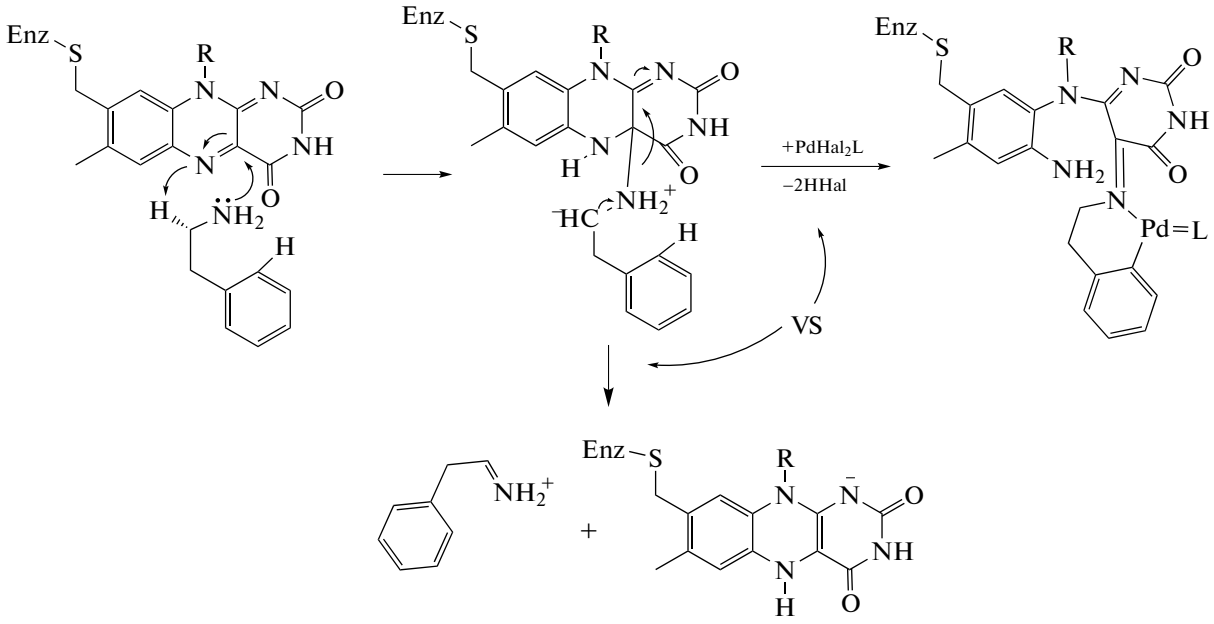

Scheme 1.

The impact of complex structure on MAO inhibition can be understood as follows. Firstly, an increase in the lipophilicity of the Pd(II) complex is advantageous for crossing the blood-brain barrier (BBB) and binding to the lipophilic catalytic site [37] of the MAO enzyme. Secondly, an increase in the size of the Pd(II) complex may not be beneficial for selective MAO-B inhibition as the catalytic cavity of MAO-B is smaller than that of MAO-A [37]. Thirdly, Pd(II) complexes must exhibit stability under physiological conditions as Pd(II) compounds tend to undergo decomposition resulting in the formation of Pd-black and/or $Pd_3(PO_4)_2$. Lastly, the ligands must stabilize the *cis*-halogen geometry of the coordination site to facilitate the mechanism presented in Scheme 1.

In our previous research, we conducted an investigation of Pd(II) pyridinimine complexes for the purpose of *ex vivo* inhibition of monoamine oxidase (MAO) enzymes [43]. Our findings revealed that the incorporation of nitro groups and substituents at the *ortho*-positions is conducive to achieving a potent inhibition of MAO enzymes.

The objective of the present study is to synthetize Pd(II) arylpyridinimine complexes containing *ortho*-substituents and a nitro group in the *para*-position of the benzene ring. Previous research, as reported in references [43, 44], revealed a modest augmentation in the inhibitory activity against monoamine oxidase (MAO) upon the transition from chloride-based complexes to Pd(II) bromide complexes. However, these studies lacked selectivity in assessing the inhibitory activity of MAO-B induced by Pd(II) compounds. In this regard, the present work focuses on investigating the MAO-B inhibitory activity of Pd(II) complexes through *ex vivo* methodologies, which have previously proven successful in the evaluation of MAO-B inhibitory activity of complexes composed of Cu(II), Zn, and Ni(II), as reported in reference [45].

EXPERIMENTAL

IR spectra were recorded using a Bruker VERTEX 80v Fourier spectrometer in vaseline oil over 4000–400 cm^{-1}. ^1H and ^{13}C NMR spectra (400 and 100 MHz, respectively) were recorded in $CDCl_3$ at 30°C (2,6-dimethyl-4-nitro-*N*-[pyridin-2-ylmethylildene]aniline (**L**) and 2,6-dinethyl-4-nitroaniline (L^4) or in DMSO-d6 at 50°C ($[PdLCl_2]$ (**I**), $[PdLBr_2]$ (**II**) using a Bruker Avance Neo 400 spectrometer with HMDS (hexamethyldisilazane) (^1H δ 0.055 ppm) and residual $CHCl_3$ (^{13}C δ 77.0 ppm) or DMSO-d6(^{13}C δ 39.6 ppm) as internal references. The mass spectrum was recorded on an Agilent Technologies 6890N/5975B instrument, HP-5ms capillary column, 30000 × 0.25 mm, 0.25 μm, evaporator temperature 260°C, temperature programming within 20–40 deg/min, carrier gas helium, 1 mL/min, mass spectra are obtained by the method of electron impact (70 eV). Melting points were determined using a PTP-2 instrument. Elemental analysis (C, H, N) was performed using a CHNS VARIO EL CUBE instrument. UV spectra were recorded in the range 200–1000 nm on an SF-2000 spectrophotometer (OKB Spektr, Russia); $l = 1$ cm. TLC was carried out on Sorbfil PTSKh-AF-A-UV plates in the system petroleum ether (40–70°C)–EtOAc 7 : 3.

The chemicals of at least chemical pure grade were used: $PdCl_2$, $[n\text{-}Bu_4N]Br$, 2-pyridinecarbaldehyde, 2,6-dimethylaniline, pharmaceutical substance kynuramine and irreversible covalent inhibitors chlorgiline (mainly MAO-A inhibitor), rasagiline and selegiline

(mainly MAO-B inhibitors) (Alfa Aesar, UK) and silica gel 0.063–0.2 mm (Macherey-Nagel, Germany). Used CH_3CN brand "0" Russian production.

***N*-(2,6-Dimethylphenyl)-4-methylbenzenesulfonamide (L^1) [46], *N*-(2,6-dimethylphenyl)-*N*-(phenylsulfotolyl)-4-methylbenzenesulfonamide (L^2)**: 8 mL (0.0650 mol) 2,6-dimethylaniline, 18.5 g (0.0970 mol) tosylchloride was refluxed in 32 mL of pyridine during 1 hour. Then the solvent was distilled off on a rotary evaporator, the residue was dissolved in EtOAc, washed with saturated NaCl solution and dried over $MgSO_4$. The products were separated by column chromatography on silica gel, eluting with petroleum ether (40–70°C)–EtOAc mixtures with increasing polarity in a ratio from 10 : 1 to 1 : 1: L^2 came out earlier than L^1 from the column, but the sequence was reversed on TLC. Yield L^1: 17.142 g (96%), Rf = 0.43, colorless powder mp. 135–136°C (petroleum ether (40–70°C)—EtOAc) (ref. [46] 134–135°C (CH_3OH)). Mass spectrum (EI, 70 eV), *m/z* (I_{rel} (%)): 276 (6), 275 (33) [M^+], 121 (10), 120 (100), 119 (6), 91 (17), 77 (8), 65 (7). Yield L^2: 0.523 g (3%), Rf = 0.31 colorless powder mp. 172–173°C (petroleum ether (40–70°C)–EtOAc). Mass spectrum (EI, 70 eV), *m/z* (I_{rel} (%)): 431 (7), 430 (14), 429 (54) [M^+], 275 (6), 274 (26), 273 (20), 211 (13), 210 (76), 209 (7), 208 (23), 196 (11), 195 (67), 194 (67), 180 (7), 154 (13), 152 (5), 151 (6), 139 (18), 120 (6), 119 (11), 118 (31), 105 (29), 104 (6), 93 (9), 92 (14), 91 (100), 89 (7), 77 (9), 65 (28), 39 (6). ^{1}H NMR spectrum (δ, ppm, *J*, Hz): 7.88 d. (4H, 3,5-Tos, *J* = 8.2), 7.30 d. (4H, 2,6-Tos, *J* = 8.2), 7.15 t. (1H, 4-Ar, *J* = 7.6), 7.01 d. (2H, 3,5-Ar, *J* = 7.6), 2.43 s. (6H, Me-Tos), 1.86 s. (6H, Me-Ar). ^{13}C NMR spectrum (δ, ppm): 145.1, 141.0, 137.1, 133.1, 129.5, 129.4, 129.4, 129.1, 21.6, 19.3. IR spectrum (ν, cm^{-1}): 3268, 1513, 1335, 1306, 1294, 1158, 1091, 814, 745, 550, 537.

For $C_{22}H_{23}NO_4S_2$

Anal. calcd., %	C, 61.51	H, 5.40	N, 3.26
Found, %	C, 61.51	H, 5.39	N, 3.46

***N*-(2,6-Dimrethyl-4-nitrophenyl)benzenesulfonamide (L^3)** [46]: 4 g (14.5 mmol) L^1, 20 mL H_2O, 30 mL CH_3COOH, 0.1 g $NaNO_2$ and 2.5 mL 60% HNO_3 was refluxed during 30 minutes. The reaction mass was cooled to 0°C and filtered on Schott, the precipitate was washed with cold water and dried under vacuum. The product was purified from residues by L^1 column chromatography on silica gel, eluting with petroleum ether (40–70°C)–EtOAc mixtures with increasing polarity in the ratio from 10 : 1 to 0 : 1: L^1 came out before L^3. Yield: 3.561 g (77%), Rf = 0.31 colorless powder mp. 150–151°C (petroleum ether (40–70°C)–EtOAc) (ref. [46] 163–165°C (H_2O)). Mass spectrum (EI, 70 eV), *m/z* (I_{rel} (%)): 321 (9), 320 (46) [M^+], 165 (28), 156 (8), 155 (88), 135 (9), 119 (18), 118 (15), 106 (5), 104 (9), 92 (10), 91 (100), 89 (5), 65 (18), 39 (6).

2,6-Dinethyl-4-nitroaniline (L^4) [46]: to 3 g (9.36 mmol) L^3 added 15 mL concentrated H_2SO_4 was stirred at 50°C during 2 houres. Then, 150 g of snow and 100 g of $NaHCO_3$ in small portions were added to the reaction mass with stirring. The solution was stirred until gas evolution ceased and extracted into EtOAc. The organic layer was dried over $MgSO_4$, filtered, and distilled off on a rotary evaporator. The residue was crystallized from CH_2Cl_2. Yield: 1.370 g (88%), green needles mp 163–164°C (CH_2Cl_2) (ref. [46] 164–165°C (EtOAc)). Mass spectrum (EI, 70 eV), *m/z* (I_{rel} (%)): 167 (10), 166 (100) [M^+], 136 (46), 120 (22), 119 (9), 118 (12), 108 (7), 104 (8), 103 (6), 93 (21), 92 (7), 91 (30), 78 (6), 77 (27), 65 (9), 52 (6), 51 (6), 39 (6). ^{1}H NMR spectrum (δ, ppm): 2.21 s. (6H, CH_3), 4.14 br.s. (2H, NH_2), s. 7.88 (2H, 3,5-Ar).

2,6-Dimethyl-4-nitro-*N*-(pyridin-2-ylmethylildene)-aniline (L): 1.274 g (7.67 mmol) L^4, 0.81 mL (8.43 mmol) 2-pyridinecarbaldehyde, 0.15 g toluenesulfonic acids was refluxed of 50 mL toluene with Dean–Stark apparatus during 12 houres. Then the solvent was distilled off on a rotary evaporator, and the residue was crystallized from CH_3OH. Yield: 1.606 g (82%), pale yellow prism mp. 155–156°C (CH_3OH). Mass spectrum (EI, 70 eV), *m/z* (I_{rel} (%)): 255 (32) [M^+], 254 (36), 241 (15), 240 (100), 237 (7), 210 (7), 209 (39), 208 (26), 207 (23), 195 (8), 164 (43), 193 (13), 192 (8), 182 (6), 181 (17), 180 (8), 160 (20), 131 (26), 130 (34), 104 (11), 103 (16), 92 (5), 80 (12), 79 (76), 78 (19), 77 (16), 65 (10), 64 (5), 63 (10), 52 (12), 51 (12), 39 (8). ^{1}H NMR spectrum (δ, ppm, *J*, Hz): 8.73 d.d.d. (1H, 6-Py, *J* = 4.9, *J* = 1.3, *J* = 0.9), 8.30 s. (1H, 7-Py), 8.25 d. (1H, 3-Py, *J* = 7.6), 7.96 s. (2H, 3,5-Ar), 7.87 d.d.d. (1H, 4-Py, *J* = 7.6, *J* = 7.5, *J* = 1.3); 7.45 d.d.d. (1H, 5-Py, *J* = 7.5, *J* = 4.9, *J* = 1.1); 2.20 s. (6H, Me). ^{13}C NMR spectrum (δ, ppm): 163.9, 156.0, 153.5, 149.8, 144.0, 136.9, 127.9, 125.9, 123.4, 121.6, 18.3. IR spectrum (ν, cm^{-1}): 3396, 1649, 1509, 1472, 1334, 1304, 1289, 1100, 764, 749.

For $C_{14}H_{13}N_3O_2$

Anal. calcd., %	C, 65.87	H, 5.13	N, 16.46
Found, %	C, 66.03	H, 5.91	N, 16.40

***cis*-Dichlorine[2,6-dimethyl-4-nitro-*N*-[pyridin-2-ylmethylildene]aniline]palladium(II) (I):** in 100 mL CH_3CN during 10 minutes was refluxed 709 mg (4 mmol) $PdCl_2$, and then added 1.021 g (4 mmol) L. The solution was refluxed for 1 hour and then filtered. The precipitate, a yellow powder, was dried in a vacuum oven. The red crystal for XRD was grown from DMSO. Yield: 1.229 g (71%), mp > 320°C (CH_3CN).

^{1}H NMR spectrum (δ, ppm, *J*, Hz): 9.12 d.d. (1H, 6-Py, *J* = 5.2), s. 8.80 (1H, 7-Py), 8.47 d.d.d. (1H, 4-Py, *J* = 8.2, *J* = 7.2, *J* = 1.0), d. 7.87 (1H, 3-Py, *J* = 7.2), s. 8.23 (2H, 3,5-Ar), d.d.d. 8.05 (1H, 5-Py, *J* = 8.2, *J* = 5.2, *J* = 1.2), 2.45 s. (6H, Me). ^{13}C NMR spectrum (δ, ppm): 175.0, 154.9, 154.9, 150.2, 145.9, 141.1, 132.8, 130.1, 129.8, 122.3, 18.0. IR spectrum (ν, cm^{-1}): 3025, 1618, 1518, 1476, 1341, 1324, 1308, 1299, 1157, 1096, 825, 765.

For $C_{14}H_{13}N_3O_2Cl_2Pd$

Anal. calcd., %	C, 38.87	H, 3.03	N, 9.71
Found, %	C, 38.37	H, 3.02	N, 9.50

***cis*-Dibromine[2,6-dimethyl-4-nitro-*N*-[pyridin-2-ylmethylildene]aniline]palladium(II) (II):** in 100 mL CH_3CN 709 mg (4 mmol) $PdCl_2$, 5.025 g (20 mmol) $BrN(Bu)_4$ and 1.021 g (4 mmol) L was refluxed during 2 houres. Then the reaction mass was evaporated on a rotary evaporator to 50 mL and cooled. The precipitate that formed was separated by filtration, washed with 50 mL of H_2O and 10 mL of CH_3CN. Yield: 1.540 g (74%), small orange crystals mp > 320°C (CH_3CN). ^{1}H NMR spectrum (δ, ppm, *J*, Hz): 9.10 br.s (1H, 6-Py), 8.78 s. (1H, 7-Py), 8.47 d.d. (1H, 4-Py, *J* = 7.2, *J* = 7.2), 8.21 d. (1H, 3-Py, *J* = 7.2), 8.04 s. (2H, 3,5-Ar), 8.01 br.s. (1H, 5-Py), 2.42 s. (6H, Me). ^{13}C NMR spectrum (δ, ppm): 174.6, 145.8, 140.8, 140.9, 132.6, 129.9, 129.6, 123.6, 122.0, 119.8, 17.9. IR spectrum (ν, cm^{-1}): 3411, 1629, 1519, 1467, 1343, 1304, 1159, 1092, 815, 763, 747, 547, 539.

For $C_{14}H_{13}N_3O_2Br_2Pd$

Anal. calcd., %	C, 32.24	H, 2.51	N, 8.06
Found, %	C, 35.44	H, 3.32	N, 8.62

X-ray. A set of experimental reflections of compound samples was obtained on an Xcalibur Ruby single-crystal diffractometer (Agilent Technologies, Poland) with a CCD detector according to the standard method (MoK_α radiation, ω-scan with a step of 1°) at *T* = 295 K. Absorption was taken into account empirically using the SCALE3 ABSPACK algorithm [47]. The structures were solved using the SHELXS program [48] and refined by the full matrix least squares method in F^2 in the anisotropic approximation for all non-hydrogen atoms using the SHELXL program [49] with the OLEX2 graphical interface [50]. Hydrogen atoms are included in the refinement in the rider model (with the exception of hydrogen atoms of the NH_2 group, which are refined independently in the isotropic approximation). The crystal of compound **II** was refined using a data file with reflection intensities of the HKLF 5 format as a twin with two components, the component ratio obtained as a result of refinement is 0.639(3) : 0.361(3). Crystallographic data and details of the refinement of structures L^4, L, **I**, and **II** are given in Table 1.

Structural data were deposited at the Cambridge Center for Crystallographic Data (nos. 2255103 (L), 2255104 (L^4), 2255106 (**I**), 2255105 (**II**), deposit@ccdc.cam.ac.uk, www: http://www.ccdc.cam.ac.uk).

Lipophilicity test. 1 L of distilled water was mixed with 60 mL of octanol-1 for two days in order to mutually saturate. 16 mg of complex **I** was stirred in 20 mL of octanol-1 saturated with water for two days, the suspension was filtered. The filtrate was made up to 30 mL with 1-octanol saturated with water. From an aliquot of the solution, the UV spectrum was recorded from 180 to 900 nm with a step of 1 nm relative to otcanol-1 saturated with water. The stock solution (20 mL) was stirred with 980 mL of water saturated with ocanol-1 for two days. Then an aliquot of the organic phase was taken to record the UV spectrum in the same way. log*P* was calculated using the formula below, where D_0 is the absorbance of the solution before extraction and D_1 is the absorbance of the solution after extraction. The calculation was carried out in the vicinity of the absorption maximum of substance **I** (263–273 nm). The log*P* values for different wavelengths were averaged, the error was calculated by Student's method with a confidence interval of 95%.

$$\log P = \log\left(\frac{D_1}{D_0 - D_1} \times \frac{980}{20}\right).$$

Stability test. 0.3 mL of a 10 mol/L solution of complex **I** in DMSO was mixed with 30 mL of 0.1 M phosphate-buffered saline (PBS) pH 7.4 and an aliquot was taken for recording the UV spectrum. The remaining solution was kept for 30 min at 37°C and an aliquot was taken to record the UV spectrum.

MTT assay. The cytotoxic activity was assayed using human cancer cell lines HEK-293 by the MTT assay. Cell cultures were incubated for 24 h in RPMI medium (PanEco, Russia) with added fetal bovine serum (10%) (Biosera, France), L-glutamine (2 mM), and 1% solution of penicillin-streptomycin (50 U/mL, 50 μg/mL; PanEco, Russia) at 37°C with 5% CO_2 in a humid atmosphere. Then, the cell cultures were treated with the tested compounds dissolved in DMSO at concentrations in the range 3.125–100 μM. Cell survival was assessed after incubation with the tested compounds for 72 h by adding MTT (3-(4,5-dimethylthiazol-2-yl)-2,5-diphenyltetrazoliumbromide) solution (20 μL, 5 mg/mL) to each well. The cells were incubated with MTT solution for 4 h. Then, the medium was removed from the plates. Each well was treated with DMSO (100 μL) to dissolve the resulting formazan crystals. The optical density was determined at 544 nm using a FLUOstar Optima plate spectrophotometer (BMG Labtech GmbH, Germany). The 50% inhibitory concentration (IC_{50}) was determined from dose-dependent curves using GraphPad Prism 6.0 software [51].

Table 1. Crystallographic parameters and details of structure refinement L^4, L, **I** and **II**

Compound	Value			
	L^4	L	**I**	**II**
Gross formula	$C_8H_{10}N_2O_2$	$C_{14}H_{13}N_3O_2$	$C_{14}H_{13}N_3O_2C_{l2}Pd$	$C_{14}H_{13}N_3O_2C_{l0.89}Br_{1.11}Pd$
M	166.18	255.27	432.57	481.70
T, K	295(2)	295(2)	295(2)	295(2)
Syngony	Monoclinic	Monoclinic	Monoclinic	Monoclinic
Space group	$P2_1/n$	$P2_1/c$	$P2_1/c$	$P2_1/c$
a, Å	3.9903(17)	8.776(2)	8.1188(13)	8.1644(14)
b, Å	11.872(4)	17.579(4)	11.2468(16)	11.495(2)
c, Å	17.149(5)	8.277(2)	17.235(2)	17.453(4)
α, deg	90	90	90	90
β, deg	92.97(4)	94.37(2)	102.542(14)	102.57(2)
γ, deg	90	90	90	90
V, Å^3	811.3(5)	1273.1(5)	1536.2(4)	1598.7(5)
Z	4	4	4	4
ρ(cal.), g/cm^3	1.360	1.332	1.870	2.001
μ, mm^{-1}	0.100	0.092	1.565	4.081
F(000)	352.0	536.0	856.0	936.0
2θ data acquisition range, deg	6.86–58.93	6.57–58.91	4.36–58.77	4.27–58.83
Independent reflections (R_{int})	2687	2993 (0.0296)	3632 (0.0298)	3790 (0.0539)
Reflections with $I > 2\sigma(I)$	1271	2223	3104	2957
Adjustable parameters	120	175	201	221
GOOF	0.916	1.039	1.055	1.021
R-factors in $F^2 > 2\sigma(F^2)$	$R_1 = 0.0748$, $wR_2 = 0.1929$	$R_1 = 0.0505$, $wR_2 = 0.1253$	$R_1 = 0.0325$, $wR_2 = 0.0727$	$R_1 = 0.0456$, $wR_2 = 0.0931$
R-factors for all reflections	$R_1 = 0.1409$, $wR_2 = 0.2138$	$R_1 = 0.0697$, $wR_2 = 0.1442$	$R_1 = 0.0406$, $wR_2 = 0.0794$	$R_1 = 0.0631$, $wR_2 = 0.1066$
$\Delta\rho_{max}/\Delta\rho_{min}$, e/Å^3	0.24/–0.20	0.21/–0.22	0.67/–0.65	0.68/–1.02

Determination of MAO inhibitory activity. The enzymatic activity of MAO in the mouse brain homogenate was determined according to the methods [52, 53] with modifications based on the fluorimetric measurement of 4-hydroxyquinoline formed during the enzymatic oxidation of kynuramine. The homogenate was prepared from mouse brain tissue in the ratio of 1 g of brain tissue to 8 mL of PBS buffer. The homogenate was centrifuged at 1000 *g* for 30 min, then the supernatant was collected and centrifuged at 10000 *g* for 30 min. Next, the pellet was resuspended in 0.01 M PBS until the protein content was 125 μg/mL. The protein concentration was determined by the Lowry method [54]. To determine the activity of MAO, a suspension of mitochondria was introduced into a 96-well black plate (SPL, Korea) at a rate of 100 μL/well and incubated at 37°C for 30 min. Prior to compound addition, MAO-A activity was suppressed by adding the selective inhibitor chlorhyline at a concentration of 250 nM per well. The test compounds in an amount of 1 μM were dissolved in 100 μL of 100% DMSO, diluted in PBS, and added to the mitochondrial suspension in such a way as to obtain the specified final concentrations of substances from 100 to 3.125 μM (DMSO concentration from 1 to 0.031%, respectively). After 30 min incubation, the enzymatic reaction was initiated by adding a nonselective substrate kynuramine (Sigma-Aldrich, USA) at a concentration of 0.2 mg/mL in PBS, 50 μL/well. Then the plates were incubated at 37°C for 30 min, after which the reaction was stopped by adding 50 μL of 10% trichloroacetic acid and 50 μL of 1 M NaOH. The fluorescence intensity of 4-hydroxyquinoline, which was formed from kynuramine, was measured at 320/380 nm using a FLUOstar Optima plate spectrophotometer (BMG Labtech, Germany). A suspension of mitochondria supplemented with DMSO to a final concentration of 1% and chlorhyline at a concentration of 250 nM was used as a positive control. Enzyme activity in the control experiment was taken as 100%. The MAO-B inhibitors rasagiline and selegelin (Sigma-Aldrich, USA) were used as reference drugs, which were added by analogy with the tested compounds. All experiments were carried out in triplicate.

The IC_{50} value was calculated as the concentration of the substance that reduces the oxidation of kynuramine by the natural mixture of MAO by 50%.

DISCUSSION

The synthesis of 2,6-dimethyl-4-nitroaniline (L^4) via the reaction between tosyl chloride and 2,6-dimethylaniline has been previously reported [46, 55]. In this study, we replicated this synthesis (Scheme 2) utilizing a staged column chromatography approach (*i*, *ii*), resulting in improved yields of pure compounds L^1 and L^3 at all stages of the process compared to those reported in the literature. Furthermore, we were able to identify a novel by-product, L^2, which was characterized using ^1H and ^{13}C NMR spectroscopy, GC-MS, and elemental analysis. Finally, the structure of L^4 was confirmed using X-ray crystallography (Fig. 1).

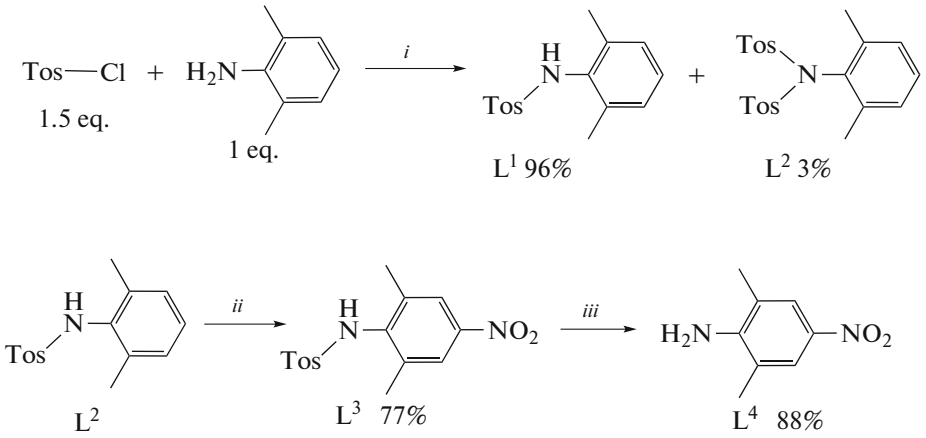

i. pyridine, refluxed, 1 h;
ii. H_2O, CH_3COOH, HNO_3, refluxed, 15 min, then Na_2CO_3;
iii. H_2SO_4, 50°C, 1 h, and then Na_2CO_3

Scheme 2.

Precursor ligand L^4 crystallizes in the centrosymmetric space group of the monoclinic system (Fig. 1). The nitro group is rotated at a small angle to the aromatic ring plane, torsion angles O(2)N(2)C(4)C(3) 3.8(5)°, O(1)N(2)C(4)C(5) 2.8(5)°. In a crystal, molecules are linked into infinite two-dimensional networks due to intermolecular hydrogen bonds N(1)–H(1A)...O(2) $(-1/2 + x, 1/2 - y, -1/2 + z)$ and N(1)–H(1B)...O(1) $(1/2 + x, 1/2 - y, -1/2 + z)$.

Schiff's base was obtained for the first time by azeotropic distillation of water 2,6-dimethyl-4-nitro-*N*-[pyridin-2-ylmethylildene)aniline (L) from priridine-2-carbaldehyde (Scheme 3). The reaction progress was monitored by TLC. The structure of the base L was proved by X-ray diffraction analysis (Fig. 2).

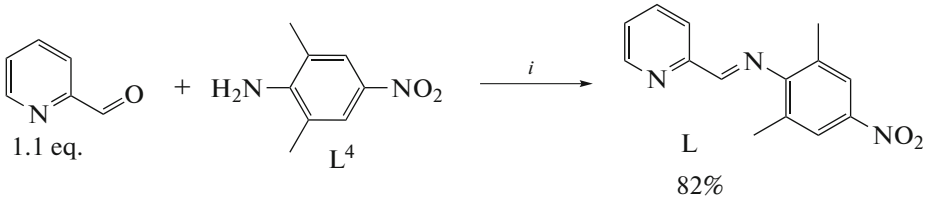

i. toluene with Dean–Stark apparatus, 10 mol % *p*-toluenesulfonic acid monohydrate, 12 h

Scheme 3.

According to X-ray data, the C(9)=N(2) double bond in compound L has the *E* configuration (Fig. 2). The nitro group, as **in** the starting amine, is rotated at a small angle to the plane of the aromatic ring, torsion

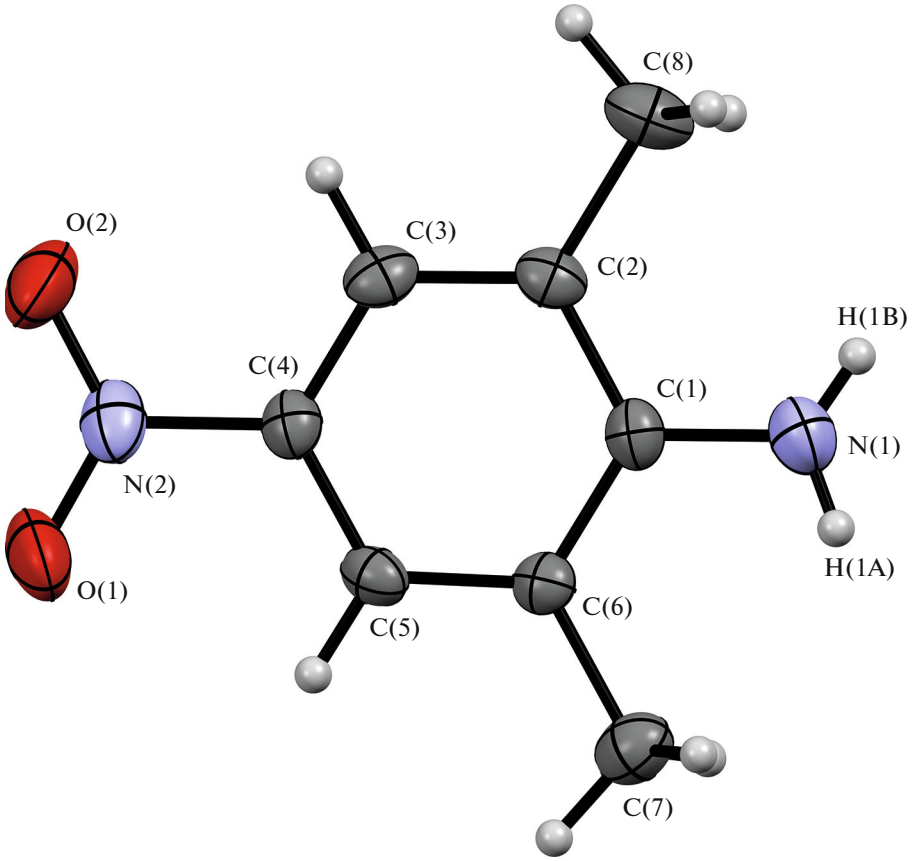

Fig. 1. General view of the molecule of compound L^4 according to X-ray diffraction data in thermal ellipsoids 30% probability.

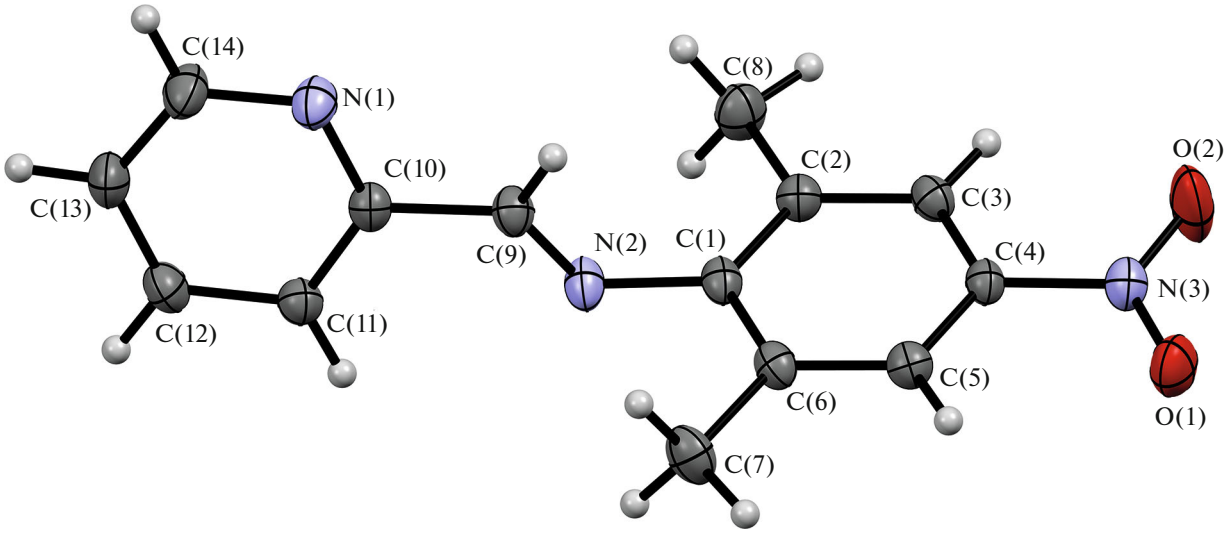

Fig. 2. General view of the molecule of compound L according to X-ray diffraction data in thermal ellipsoids 30% probability.

angles O(1)N(3)C(4)C(5) 5.7(2)°, O(2)N(3)C(4)C(3) 6.8(2)°. The angle between the C(9)N(2)C(1) plane of the imino fragment and the planes of the aryl and pyridine rings is 88.1° and 15.8°, respectively.

From the Schiff base L, the Pd(II) pyridinimine chloride complex $[PdLCl_2]$ (**I**) and the Pd(II) pyridinimine bromide complexes $[PdLBr_2]$ (**II**) were obtained for the first time (Scheme 4).

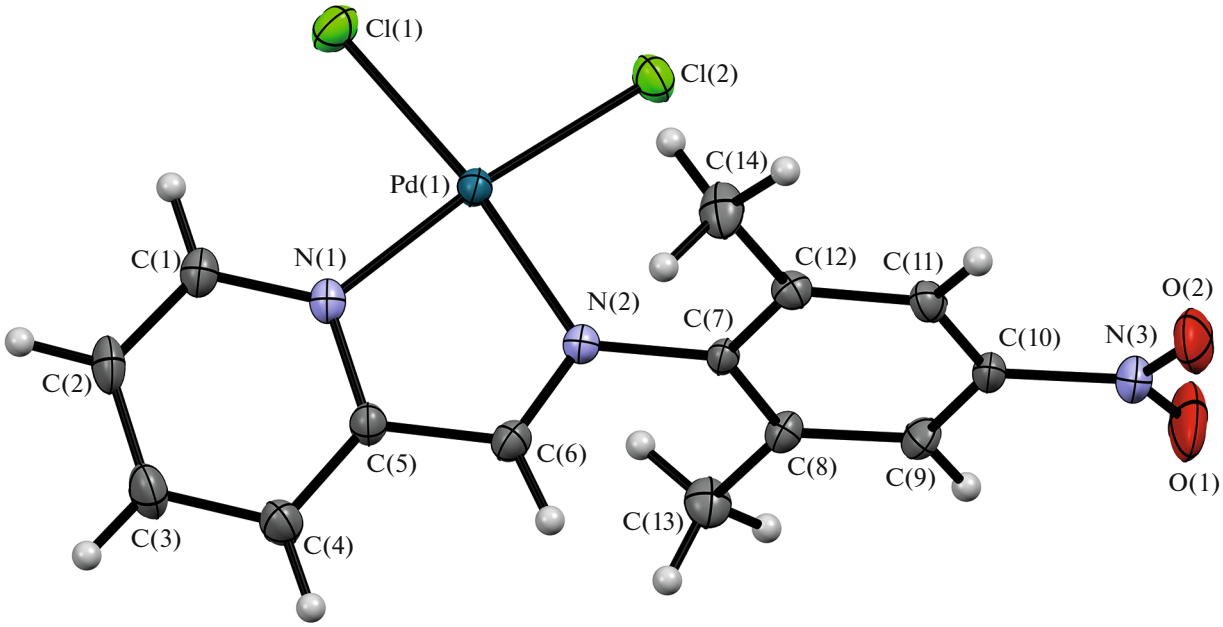

Fig. 3. General view of the molecule of compound **I** according to X-ray diffraction data in thermal ellipsoids 30% probability.

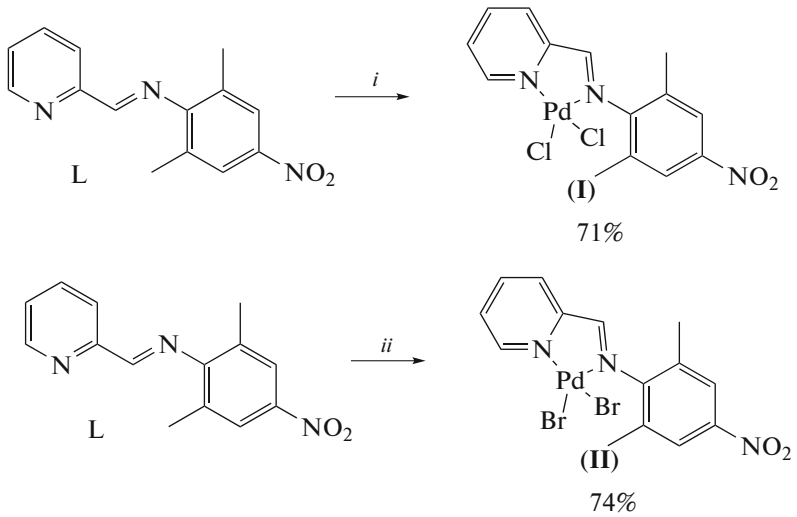

i. 1 equivalent $PdCl_2$, CH_3CN, boiling, 2 h;
ii. 1 equivalent $PdCl_2$, 4 equivalent [*p*-Bu_4N]Br, CH_3CN, refluxed, 2 h

Scheme 4.

The structures of complexes **I** and **II** were confirmed by X-ray (Figs. 3 and 4).

Complex **I** crystallizes in the centrosymmetric space group of the monoclinic system (Fig. 3). The Pd atom has a somewhat distorted flat-square environment. The Pd–N (2.02–2.03 Å) and Pd–Cl (2.27–2.28 Å) bond lengths take values typical of such complexes [56–58]. The Pd atom is deviated from the plane of the remaining four atoms of the palladacycle by 0.25 Å. The bulky aryl substituent is rotated at a large angle to the N(1)C(5)C(6)N(2) plane: the dihedral angle is 72°.

Complex **II** is an isomorph of complex **I**. The differences in the lengths of the ribs lie within 0.04–0.25 Å (Table 1). The unit cell volume of bromine-containing complex **II** (1598.7(5) $Å^3$) is larger than that of chlorine-containing complex **I** (1536.2(4) $Å^3$). Complex **II** contains a mixture of bromine and chlorine atoms in a ratio of 1.11 : 0.89, obtained as a result of structure refinement taking disorder into account. As a whole, complexes **II** and **I** have similar geometries.

The solubility and stability were studied using substance **I** as an example. Solubility at 20°C in water and

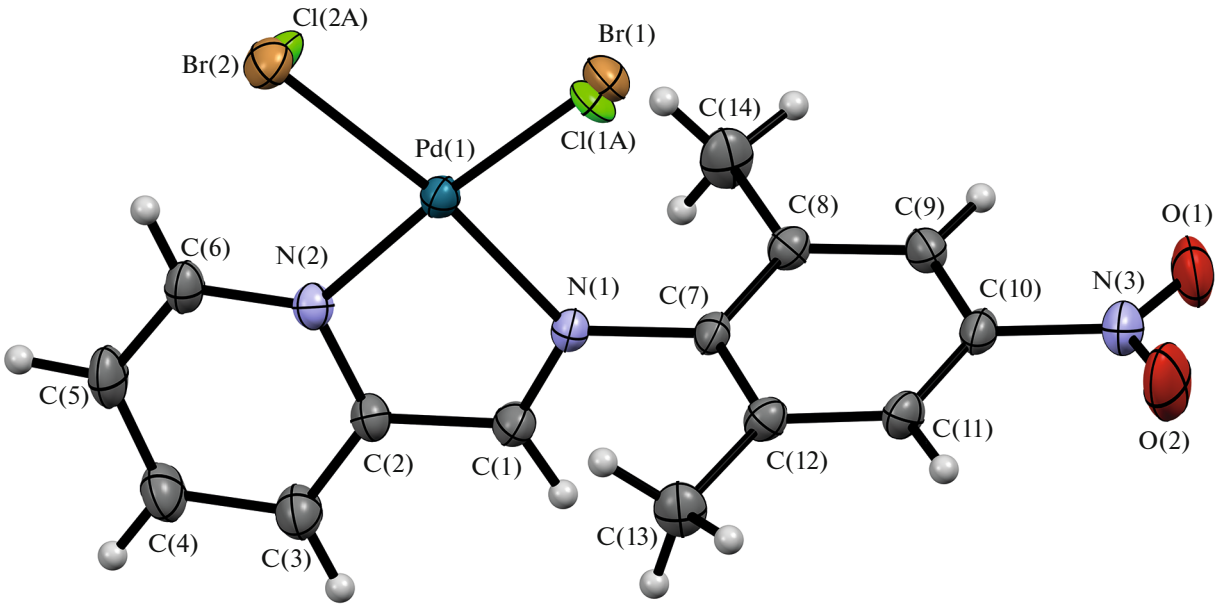

Fig. 4. General view of the molecule of compound **II** according to X-ray diffraction data in thermal ellipsoids 30% probability.

octanol-1 is less than 1 mmol L^{-1}, and in DMSO about 9 mmol L^{-1}. Boiling in water leads to decomposition with the formation of a palladium mirror. Heating in octanol-1 at 65°C leads to decomposition with the formation of Pd-black. Storing the solution in octanol-1 for a month at room temperature also leads to decomposition with the formation of Pd-black. Boiling in DMSO does not lead to visible decomposition. Additionally, resistance to DMSO was confirmed by the NMR method: keeping the solution in DMSO-d_6 for 3 days at 37°C does not lead to changes in the ^{1}H NMR spectrum recorded at a temperature of 50°C and a concentration of 100 mmol L^{-1}. Additionally, the stability of the Pd complex in PBS solution was checked; as a result of the study, the formation of palladium black and $Pd_3(PO_4)_2$ was not observed. Keeping a 0.1 mol/L solution in PBS at 37°C for 30 min did not change the UV spectrum (λ_{max} = 230 nm logε = 4.1), which confirms the stability of the complex under the conditions of the study of MAO inhibitory activity.

Using complex **I** as an example, the lipophilicity in the octanol-1/water system was studied. log$P$ = 2.08 ± 0.13, which is close to the lipophilicity value of rasagelin 2.01 [59], it is likely that the Pd complex is able to cross the BBB and interact with the MAO catalytic site. Lipophilicity was also modeled using the SwissADME program (log$P$ = 2.11). Compounds L, **I** and

Table 2. MAO-B inhibitory activity of ligand L complexes **I–IX** selegiline and rasagiline tested in mouse brain

Compound	IC_{50} concentration, μM
L	>100
I	>100
II	>100
III	19.47 ± 2.35
IV	56.34 ± 2.13
V	12.69 ± 2.35
VI	30.60 ± 4.24
VII	98.84 ± 5.63
VIII	>100
IX	>100
Selegiline	8.31 ± 1.79
Rasagiline	3.86 ± 0.51

II showed no cytotoxic activity ($IC_{50} \geq 100$ μM) against HEK-293 cells.

Ligand L and complexes **I** and **II** were studied in mouse brain homogenate (BM). The MAO enzyme is present in the brain as two isoforms: MAO-A and MAO-B in a ratio of 20 : 80% [39]. The activity of the MAO-A enzyme was inhibited by chlorgiline at a concentration of 250 nM per well. Residual MAO activity in BM was considered MAO-B activity. The inhibitors rasagelin and selegelin were used as positive controls [60]. Previously published complexes **III–VI** [43], which showed the highest non-selective activity against MAO, as well as complexes **VII–IX** [61], obtained from catecholamines (MAO substrates), and were tested for the first time for selective MAO-B inhibitory activity (Fig. 5). Table 2 shows the values of 50% inhibitory concentration (IC_{50}) of the residual activity of MAO-B in the presence of substances L, **I–IX** or reference drugs—selegiline and rasagelin.

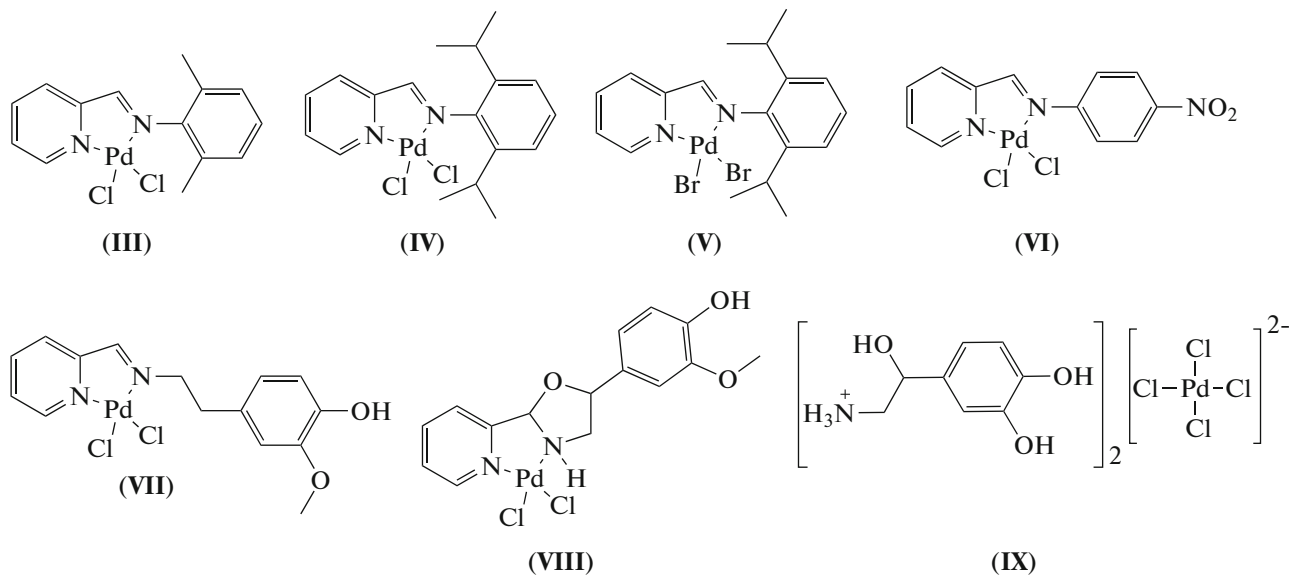

Scheme 5.

Analyzed were the structure–activity relationships in a series of synthesized Pd(II) complexes, from which the following patterns were discovered:

(1) The inclusion of a nitro group into the *para*-position of the benzene ring demonstrated the inhibition of the MAO-B activities of complex **I** in comparison to complex **III**.

(2) The expansion in the scale of the substituent located in the *ortho*-position of the benzene ring was correlated with a decrease in MAO-B inhibitory activity as observed in complexes **I** versus **VI**, and **III** versus **IV**.

(3) The substitution of chlorides with bromides was noted to increase the MAO-B inhibitory activity of complex **V** when compared to complex **IV**.

These relationships will be employed in the development of future Pd(II) complex synthesis and the identification of the mechanisms responsible for MAO-B inhibitory activity. To fully comprehend the inhibitory effects on MAO-A and MAO-B, it is necessary to examine the degree of inhibition on pure enzymes in vitro. Additionally, the impact on GABA biosynthesis in astrocytes and the cytotoxic activity of the Pd(II) complexes pertaining to neuronal precursors and astrocytes warrants investigation.

ACKNOWLEDGMENTS

The work was carried out using the equipment of The Core Facilities Centre "Research of materials and matter" at the PFRC UB RAS. The author acknowledges O.A. Maiorova (Perm Federal Research Center, Ural Branch, RAS) for recording the NMR spectra, I.A. Borisova (Perm Federal Research Center, Ural Branch, RAS) for recording the IR spectra, M.V. Dmitriev for X-ray (Perm State University), A.A. Gorbunov for GC-MS and A.O. Voronina and O.N. Gagarskikh (Perm Federal Research Center, Ural Branch, RAS) for performing the MTT test.

FUNDUNG

The study was supported by the Russian Foundation for Basic Research and the Perm Region Ministry of Education and Science according to the Research Project no. 19-43-590003.

CONFLICT OF INTEREST

The authors of this work declare that they have no conflicts of interest

REFERENCES

1. Ndagi, U., Mhlongo, N., and Soliman, M.E., *Drug Des. Dev. Ther.*, 2017, vol. 11, p. 599. https://doi.org/10.2147/DDDT.S119488
2. Kotieva, I.M., Dodokhova, M.A., Safronenko, A.V., et al., *J. Clin. Oncol.*, 2022, vol. 40, no. 16, p. e15080. https://doi.org/10.1200/JCO.2022.40.16_suppl.e15080
3. Yambulatov, D.S., Lutsenko, I.A., Nikolaevskii, S.A., et al., *Molecules*, 2022, vol. 27, no. 23, p. 8565. https://doi.org/10.3390/Molecules27238565
4. Czarnomysy, R., Radomska, D., Szewczyk, O.K., et al., *Int. J. Mol. Sci*., 2021, vol. 22, no. 15, p. 8271. https://doi.org/10.3390/ijms22158271
5. Abu-Surrah, A.S. and Kettunen, M., *Curr. Med. Chem.*, 2006, vol. 13, no. 11, p. 1337.
6. Sharma, N.K., Ameta, R.K., and Singh, M., *Biochem. Res. Int.*, 2016, vol. 2016. 4359375. https://doi.org/10.1155/2016/4359375
7. Scattolin, Th., Voshkin, V.A., Visentin, F., and Nolan, S.P., *Cell. Rep. Phys. Sci.*, 2021, vol. 2, p. 100446. https://doi.org/10.1016/j.xcrp.2021.100446
8. Boyarskii, V.P., Mikherdov, A.S., Baikov, S.V., et al., *Pharm. Chem. J.*, 2021, vol. 55, no. 2, p. 130. https://doi.org/10.1007/s11094-021-02393-1
9. Batyrenko, A.A., Mikolaichuk, O.V., Ovsepyan, G.K., et al., *Russ. J. Gen. Chem.*, 2021, vol. 91, no. 4, p. 666. https://doi.org/10.1134/S1070363221040149
10. Zalevskaya, O.A., Gur'eva, Y.A., and Kutchin, A.V., *Inorg. Chim. Acta*, 2021, vol. 527, p. 120593. https://doi.org/10.1016/j.ica.2021.120593
11. Ibatullina, M.R., Zhil'tsova, E.P., Kulik, N.V., et al., *Russ. Chem. Bull.*, 2022, vol. 71, no. 2, p. 314. https://doi.org/10.1007/s11172-022-3413-6
12. Denisov, M.S. and Glushkov, V.A., *Bull. Perm. Univ. Chem.*, 2018, vol. 8, no. 4, p. 388. https://doi.org/10.17072/2223-1838-2018-4-388-411
13. Egorova, K.S., Galushko, A.S., and Ananikov, V.P., *Angew. Chem., Int. Ed. Engl.*, 2020, vol. 59, p. 22296. https://doi.org/10.1002/anie.20200308
14. Denisov, M.S., *Vestn. Perm. Feder. Issl. Tsentr.*, 2021, no. 4, p. 6. https://doi.org/10.7242/2658-705X/2021.4.1
15. Patra, M. and Gasse, G., *ChemBioChem*, 2012, vol. 13, no. 9, p. 1232. https://doi.org/10.1002/cbic.201200159
16. Özbek, N., Alyar, S., Memmi, B.K., et al., *J. Mol. Struct.*, 2017, vol. 1127, p. 437. https://doi.org/10.1016/j.molstruc.2016.07.122
17. Ahmed, M., Khan, Sh.Z., Sher, N., et al., *J. Venomous Anim. Toxins Incl. Trop. Dis.*, 2021, vol. 27, p. e20200047. https://doi.org/10.1590/1678-9199-JVATITD-2020-0047
18. Bal, S., Demirci, Ö., Şen, B., et al., *Polyhedron*, 2021, vol. 198, p. 115060. https://doi.org/10.1016/j.poly.2021.115060
19. Sahin, Ö., Özdemir, Ü.Ö., Seferoğlu, N., et al., *J. Biomol. Struct. Dyn.*, 2021, p. 4460. https://doi.org/10.1080/07391102.2020.1858163
20. García-García, A., Rojas, S., Rivas-García, L., et al., *Chem. Commun.*, 2022, vol. 58, p. 1514. https://doi.org/10.1039/D1CC04404D
21. Karataş, M.O., Çalgın, G., Alıcı, B., et al., *Appl. Organomet. Chem.*, 2019, vol. 33, no. 10, p. e5130. https://doi.org/10.1002/aoc.5130
22. Asma, M., Badshah, A., Ali, S., et al., *Transition Met. Chem.*, 2006, vol. 31, p. 556. https://doi.org/10.1007/s11243-006-0027-z
23. Lassig, J.P., Shultz, M.D., Gooch, M.G., et al., *Arch. Biochem. Biophys.*, 1995, vol. 322, no. 1, p. 119. https://doi.org/10.1006/abbi.1995.1443
24. Vieites, M., Smircich, P., Parajón-Costa, B., et al., *J. Biol. Inorg. Chem.*, 2008, vol. 13, no. 10, p. 1839. https://doi.org/10.1016/j.jinorgbio.2008.05.010
25. Fricker, S.P., Mosi, R.M., Cameron, B.R., et al., *J. Inorg. Biochem.*, 2008, vol. 102, no. 10, p. 1839. https://doi.org/10.1016/j.jinorgbio.2008.05.010
26. Carneiro, Z.A., Lima, J.C., Lopes, C.D., et al., *Eur. J. Med. Chem.*, 2019, vol. 180, no. 15, p. 213. https://doi.org/10.1016/j.ejmech.2019.07.014
27. Gama, N.H., Elkhadir, A.Y.F., Gordhan, B.G., et al., *Biometals*, 2016, vol. 29, p. 637. https://doi.org/10.1007/s10534-016-9940-6
28. Chen, Ch., Sun, L.-Yu., Gao, H., et al., *ACS Infect. Dis.*, 2020, vol. 6, no. 5, p. 975. https://doi.org/10.1021/acsinfecdis.9b00385
29. Mital, R., Shah, G.M., Srivastava, T.S., and Bhattacharya, R.K., *Life Sci.*, 1992, vol. 50, no. 11, p. 781. https://doi.org/10.1016/0024-3205(92)90183-P
30. Petrović, Z.D., Hadjipavlou-Litina, D., Pontiki, E., et al., *Bioorg. Chem.*, 2009, vol. 37, no. 5, p. 162. https://doi.org/10.1016/j.bioorg.2009.07.003
31. Hegazy, W.H. and Al-Faiyz, Ya.S., *Med. Chem. Res.*, 2014, vol. 23, no. 1, p. 518. https://doi.org/10.1007/s00044-013-0661-x
32. Lima, M.A., Costa, V.A., Franco, M.A., et al., *Inorg. Chem. Commun.*, 2020, vol. 112, p. 107708. https://doi.org/10.1016/j.inoche.2019.107708
33. Krinulović, K., Bugarčić, Ž., Vrvić, M., et al., *Toxicol. In Vitro*, 2006, vol. 20, no. 8, p. 1292. https://doi.org/10.1016/j.tiv.2006.03.002
34. Tatyanenko, L.V., Kotelnikova, R.A., Zakharova, I.A., and Moshkovskii, Yu.Sh., *Inorg. Chim. Acta*, 1981, vol. 56, p. 89.
35. Parrilha, G.L., Ferraz, K.S.O., Lessa, J.A., et al., *Eur. J. Med. Chem.*, 2014, vol. 84, no. 12, p. 537. https://doi.org/10.1016/j.ejmech.2014.07.055
36. Türkan, F., Huyut, Z., and Atalar, M.N., *J. Biochem. Mol. Toxicol.*, 2018, vol. 32, no. 10, p. e22205, https://doi.org/10.1002/jbt.22205
37. Edmondson, D.E., Binda, C., and Mattevi, A., *Arch. Biochem. Biophys.*, 2007, vol. 464, p. 269. https://doi.org/10.1016/j.abb.2007.05.006
38. *Pharmaceutical Chemistry*, Watson, D.R., Ed., Glasgow: Elsevier, 2011, p. 641.
39. Hong, R. and Li, X., *MedChemComm*, 2019, vol. 10, p. 10. https://doi.org/10.1039/c8md00446c
40. Tat'yanenko, L.V., Sokolova, N.V., and Moshkovsky, Y.S., *Vopr. Med. Khim.*, 1982, vol. 28, p. 126.
41. Albert, J., Cadena, J.M., González, A., et al., *Chem. Commun.*, 2003, vol. 41, no. 4, p. 528. https://doi.org/10.1039/B211808D

42. Cho, H.-U., Kim, S., Sim, J., et al., *Exp. Mol. Med.*, 2021, vol. 53, p. 1148. https://doi.org/10.1038/s12276-021-00646-3
43. Denisov, M.S., Gagarskikh, O.N., and Utushkina, T.A., *Bull. Perm. Univ. Chem.*, 2021, vol. 11, no. 1, p. 30. https://doi.org/10.17072/2223-1838-2021-1-30-58
44. Denisov, M.S., Dmitriev, M.V., Eroshenko, D.V., et al., *Russ. J. Inorg. Chem.*, 2019, vol. 64, no. 1, p. 56. https://doi.org/10.1134/S0036023619010054
45. Yang, D.D., Wang, R., Zhu, J.L., et al., *J. Mol. Struct.*, 2017, vol. 1128, no. 15, p. 493. https://doi.org/10.1016/j.molstruc.2016.08.037
46. Hao, Ch., Huang, W., Li, X., et al., *Eur. J. Med. Chem.*, 2017, vol. 131, p. 1. https://doi.org/10.1016/j.ejmech.2017.02.063
47. *CrysAlisPro. Agilent Technologies. Version 1.171.37.33* (release 27-03-2014 CrysAlis171 .NET).
48. Sheldrick, G.M., *Acta Crystallogr., Sect. A: Found. Crystallogr.*, 2008, vol. 64, p. 112. https://doi.org/10.1107/S0108767307043930
49. Sheldrick, G.M., *Acta Crystallogr., Sect. C: Struct. Chem.*, 2015, vol. 71, p. 3. https://doi.org/10.1107/S2053229614024218
50. Dolomanov, O.V., Bourhis, L.J., Gildea, R.J., et al., *J. Appl. Crystallogr.*, 2009, vol. 42, p. 339. https://doi.org/10.1107/S0021889808042726
51. Gonçalves, B.M.F., Salvador, J.A.R., Marín, S., and Cascante, M., *Eur. J. Med. Chem.*, 2016, vol. 114, p. 101. https://doi.org/10.1016/j.ejmech.2016.02.057
52. Thull, U. and Testa, B., *Biochem. Pharmacol.*, 1994, vol. 47, no. 22, p. 2307. https://doi.org/10.1016/0006-2952(94)90271-2
53. Andrade, J.M.M., Passos, C.D.S., Dresch, R.R., et al., *Pharmacogn. Mag.*, 2014, vol. 10, no. 37, p. 100. https://doi.org/10.4103/0973-1296.127354
54. Lowry, O.H., Rosebrough, N.J., Farr, A.L., and Randall, R.J., *J. Biol. Chem.*, 1951, vol. 193, no. 1, p. 265.
55. O'Donnell, A.D., Gavriel, A.G., Christie, W., et al., *Arkivoc*, 2021, Pt. VI, p. 222. https://doi.org/10.24820/ark.5550190.p011.581
56. Park, S., Lee, J., Jeong, J.H., et al., *Polyhedron*, 2018, vol. 151, no. 1, p. 82. https://doi.org/10.1016/j.poly.2018.05.031
57. Motswainyana, W.M., Onani, M.O., Jacobs, J., and Meervelt, L.V., *Acta Crystallogr. Sect. C: Cryst. Struct. Commun.*, 2012, vol. 68, p. 356. https://doi.org/10.1107/S0108270112045970
58. Laine, T.V., Klinga, M., and Leskelä, M., *Eur. J. Inorg. Chem.*, 1999, vol. 1999, no. 6, p. 959. https://doi.org/10.1002/(SICI)1099-0682(199906)1999:6<959::AID-EJIC959>3.0.CO;2-Z
59. Delogu, G.L., Pintus, F., Mayán, L., et al., *MedChemComm*, 2017, vol. 8, p. 1788. https://doi.org/10.1039/C7MD00311K
60. Finberg, J.P.M. and Rabey, J.M., *Front. Pharmacol.*, 2016, vol. 18, no. 7, p. 340. https://doi.org/10.3389/fphar.2016.00340
61. Denisov, M.S. and Gagarskikh, O.N., *Russ. J. Gen. Chem.*, 2021, vol. 91, no. 7, p. 1354. https://doi.org/10.1134/S1070363221070136